UV Thermal Imaging of RF GaN Devices with GaN Resistor Validation

Dustin Kendig[1], Georges Pavlidis[2], Samuel Graham[2], Justin Reiter[3], Michael Gurr[4], David Altman[4], Stephen Huerster[4], Ali Shakouri[5]

[1]Microsanj, LLC, Santa Clara, CA, [2]Georgia Institute of Technology, Atlanta, GA, [3]Analog Devices, Norwood, MA, [4]Raytheon Corporation, Waltham, MA, [5]Purdue University, West Lafayette, IN

Abstract— **Shrinking features and growing device complexity in advanced microwave devices has increased the challenge of fully understanding device thermal behavior on the sub-micron scale. Predicting the device static and dynamic thermal behavior is essential for ensuring optimal tradeoffs between performance and device reliability. Thermal imaging based on the Thermoreflectance Principle can meet the challenges imposed by these compact, high power density RF devices by providing sub-micron spatial resolution and temporal resolution in the picosecond range. This technique overcomes the limitations of traditional thermal imaging techniques such as IR and Micro-Raman and some of the specific challenges in measuring GaN devices. In the past, Thermoreflectance Imaging has been shown to accurately estimate the temperature rise of metals using visible wavelength excitation sources. This paper presents a novel method to estimate the temperature directly on GaN surfaces using UV wavelengths. These UV thermoreflectance measurements were verified with measurement of an on-chip GaN mesa resistor. Temperature measurements on top of the field plate and inside the GaN channel were compared for a commercial GaN HEMT both on Si and SiC substrate. The advantages and disadvantages will be presented for the thermoreflectance technique for thermal imaging.**

Index Terms— **Thermoreflectance thermal imaging, IR thermography, GaN HEMT**

I. INTRODUCTION

The use of wide band-gap semiconductors [1] in high frequency transistors for communications and power devices has increased significantly over the past 20 years. In parallel, thermal consideration in chip design has become a large concern [2] in addition to the thermal packaging [3]. To take advantage of high speed switching and construct Monolithic Microwave Integrated Circuits (MMICs), the feature length of the transistor gate has been reduced to few tens of nanometers. Consequently, this has made thermal characterization of each individual transistor increasingly more difficult [4].

Thermal characterization of GaN and other wide-bandgap semiconductors has some unique challenges compared to Si and GaAs. The wide bandgap leads to transparency and thin film interference issues which can lead to errors in optical techniques like IR [5], Micro-Raman [6], and Thermoreflectance [7]. For IR measurements, a device with 2 µm of GaN and 200 µm of SiC is 75-85% transparent and has an emissivity ~0.85 [7]. This can lead to IR emission from deep below the surface to reach the IR detector. Gold metallization on the back contact can reflect more radiation and lead to errors between the calibration and measurement. Adding black paint can typically help with these transparency and emissivity issues, but these paints can be thick and affect the electrical performance under RF Operation.

Micro-Raman spectroscopy overcomes some of the limitations for spatial resolution by using a visible [4] or UV light [8] laser to measure the temperature dependent Raman shift of the material. For GaN, sub-bandgap lasers provide a depth averaged temperature rise while UV Raman can be used to obtain the temperature at the top surface of the device. Precautions must be taken, however, to ensure that the high laser power does not damage the device when creating electron-hole pairs in the channel [8]. The main obstacle with Raman is typically highlighted when evaluating devices with metal field plates which obstruct Raman measurements taken near the gate edge. Measurements must be made in the optically accessible GaN channel and thus not directly in the hot spot region. Potential solutions to this problem has been proposed by performing Raman measurements from the backside [7] or placing nanoparticles on the surface [9] to overcome these issues.

Recent developments have made it possible to characterize the surface temperature of such circuits using a CCD-based thermoreflectance (TR) thermal imaging method [10]. The underlying principle behind TR imaging can be expressed by (1):

$$\frac{\Delta R(x,y,\lambda)}{R(x,y,\lambda)} = \Delta C_{th}(x,y,\lambda)\Delta T \qquad (1)$$

The intensity of the optical reflection of an illumination ($\Delta R/R$) changes with a change in surface temperature (ΔT) and can be related by the thermoreflectance coefficient, C_{th}. The C_{th} can be considered to be constant over a wide temperature range [11].

Due to the diffraction limit, which is defined by the optical properties of the microscope objective, optical and thermal images of features smaller than 300 nm blur. In [12], the impact of diffraction limit on thermal images of sub-diffraction device features is addressed, both qualitatively and quantitatively. An algorithm to predict the effect of diffraction on thermoreflectance thermal imaging of sub-diffraction devices with known shape and size is proposed. Other than diffraction, thermal expansion of the device may also lead to defocusing and subsequent blurring of thermal images. A three-dimensional piezoelectric stage controller helps to stabilize the focused location in the microscope [10]. Taking the pixel-by-pixel TR coefficients allows us to calibrate the light intensity to the temperature information precisely in targeted locations [10]. With this configuration, thermal imaging for wires with one-pixel width, ~100 nm, is achieved.

Most TR measurements use standard visible light microscopes due to the simplicity of the optics [11]. Pushing further into UV wavelengths can require special fused silica or UV anti-reflective coating objectives to improve light transmission and reduce optical aberrations [13]. By using UV light <370nm we can reduce any transmission through GaN and SiC, which can cause thin-film interference effects that convolute the thermoreflectance signal. With 365nm light, a clear reflection off of the top surface for GaN on SiC is achieved. Overall, using illumination wavelengths in the UV and visible range (365 nm to 760 nm) results in a diffraction limited spatial resolution on the order of hundreds of nanometers (260 nm for UV illumination).While submicron spatial resolution is readily achievable with TR imaging, IR thermography and Micro-Raman are limited to 3-5 µm and ~0.8-1 µm [4] respectively.

II. Thermal Measurements on GaN Resistor

To verify the UV thermoreflectance measurements, an 18 µm long by 11 µm wide GaN mesa resistor was used. The resistor temperature curve was calibrated by placing the device on a thermal chuck and measuring the resistance versus temperature using a 4-wire method.

Thermoreflectance measurements were made on the GaN resistor with a 365 nm LED and 60X/0.7NA objective coated for UV light transmission. The TR measurements were calibrated using a thermal chuck with XYZ piezoelectric control to correct for thermal expansion during cycling. The thermoreflectance material coefficient for GaN at 365nm was measured to be -1.75 x10^{-3} °C^{-1}. This is ~10x larger than typical coefficients which improves the temperature sensitivity to 5-10 mK. The resistance and TR measurements agreed to within 0.9%. Modeling, resistance, and TR measurements all agreed withing 1%. Future improvements could include measurements with 340 nm light to get further away from the GaN bandgap edge and reduce any UV light transmission from the broadband LED. A visible cut-off filter >370nm might also be used to remove the longer wavelengths that can penetrate through GaN and SiC.Thermal Analysis of GaN Transistor

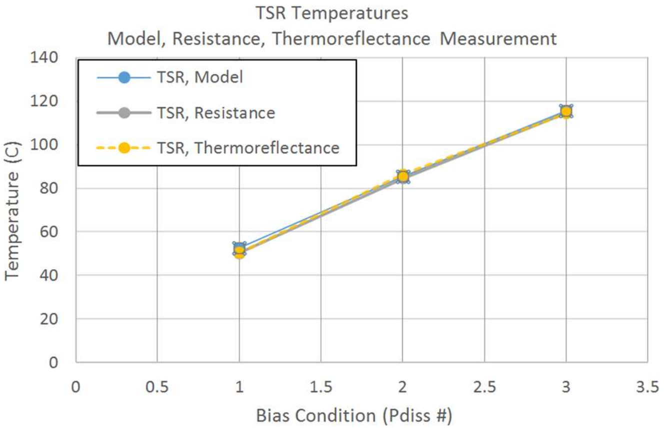

Fig. 1: Plot of the temperature sense resistor (TSR) average temperature at three different power conditions for Modeling, Resistance, and Thermoreflectance

To further assess the application of UV TR on GaN HEMTs, a UV/Visible comparison was performed on an unpassivated 2x45 µm GaN/Si HEMTs. The absence of passivation was intended to reduce the effect of thin film interference. Calibrations were performed to extract the thermoreflectance coefficient for wavelength sources of 365 nm, 470 nm and 530 nm. For a 100 °C temperature rise, the coefficients were determined to be -7x10^{-4} °C^{-1}, 1.75 x10^{-4} °C^{-1}, and -2x10^{-4} °C^{-1} respectively. A 50x/0.5NA objective was used for all wavelengths in addition to placing a 365 nm bandpass filter in the LED path for the UV TR measurements.

The transient thermal performance of these devices was assessed using transient TR. The devices were pulsed for 50 µs pulsed at a 25% duty cycle. A 20 V drain bias was applied with a negative gate bias which resulted in a peak power dissipation

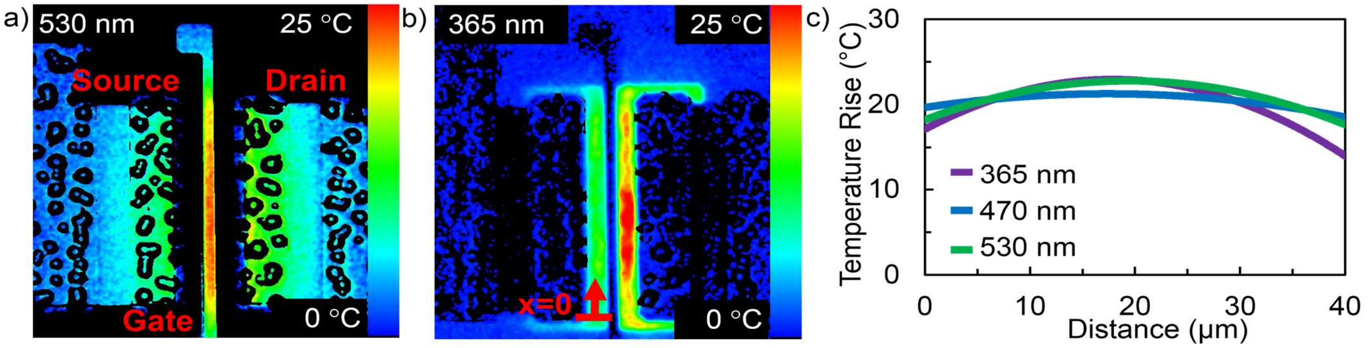

Fig. 2: Thermoreflectance (TR) image of GaN/Si HEMT showing the temperature rise of a) the gate metal using a 530 nm excitation source and b) the GaN channel using a 365 nm excitation source. c) line profiles of the temperature rise along the gate width for both visible and UV excitation sources

of 1.6 W/mm. Measurements were taken every 5 µs for an LED pulse width varying from 650 ns (visible TR) to 2.5 µs (UV TR).

The thermal images obtained from the 365 nm and 530 nm sources are shown in Figure 1a and 1b. Due to the absence of a field plate, a direct temperature comparison of the gate metal to the GaN region can be obtained. A line plot was extracted along the gate width directly over the gate metal for the visible wavelengths and was contrasted to the GaN temperature rise between the Gate and the Drain (Figure 1c). The temperature rise and profile across the gate metal agrees well between the 470 nm and 530 nm plots confirming the accuracy of these measurements. For UV TR, the temperature rise of the GaN region is also shown to be on the same order of magnitude as the gate metal but shows a more parabolic temperature profile. Specifically, the temperature rise between the center and the edge appear to be 10 °C in the GaN whereas only a 5 °C temperature gradient is observed in the Gate metal. This discrepancy can be attributed to the heat spreading in the GaN which is not possible in the Gate metal due to its geometry.

UV TR measurements were then applied to a commercial 0.25 µm GaN/SiC HEMT devices in the GaN channel region and compared to visible 530 nm measurements made on top of the field plate. A schematic of the different regions probed according to the wavelength source is shown in Figure 2.

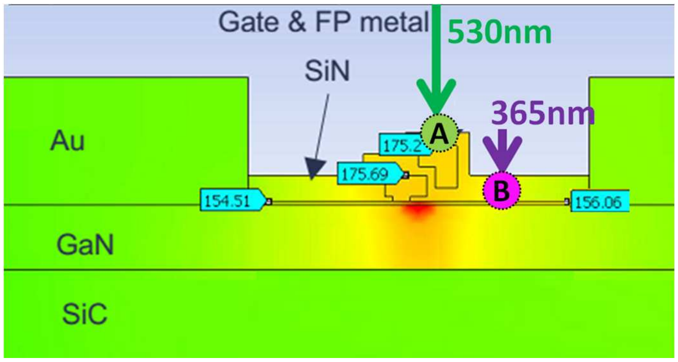

Fig. 3: Thermoreflectance measurements made on A) Top of Field Plate and B) GaN Channel. Thermal simulation data provided from [14]

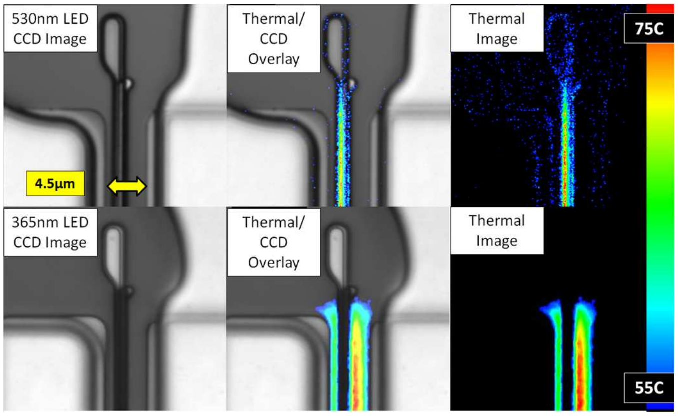

Fig. 4. a) Optical CCD Image of GaN/SiC HEMT using a 530nm and 365nm wavelengths source b) Thermal Image overlay on CCD c) Thermal Image showing temperature rise with scale adjusted to highlight heating location

Visible TR measurements made on top of the gold field plate with 530 nm light provide a clear reflection off the metal surface (Figure 3). This can provide an accurate calibration point for thermal models which can assist in determining the hotspot temperature. With a 100X/0.8NA objective the resolving power is 0.40 µm based on the Rayleigh Criterion. The NT210B Thermoreflectance system has 45nm/pixel at 100X.

UV TR measurements were made to the side of the field plate inside the GaN channel (Figure 3). Shadowing from the field plate and gate edge can block the hot spot on the Gate-Drain edge, so the temperature measurement must be made a few 100 nm away. With the 60X/0.7NA objective the resolving power is 0.32 µm and 75nm/pixel.

III. CONCLUSION

UV thermoreflectance measurements have been shown to agree well with a GaN mesa resistor temperature sensor within 0.9%. Further measurements on an active GaN HEMT device show similar temperatures between measurements on top of the gold field plate and to the side in the GaN channel. Sharp temperature gradients in the GaN channel cause the temperature measurements in the channel region to be lower than the true temperature on the Gate-Drain edge. Close thermal contact between the heat generation region and gate/field plate region continue to make these regions good choices for temperature measurement locations.

REFERENCES

[1] D. Liu, U. Pfeiffer, J. Grzyb, and B. Gaucher, *Advanced millimeter-wave technologies: antennas, packaging and circuits*: John Wiley & Sons, 2009.

[2] L. Li, R. Coccioli, K. Nary, and P. Canfield, "Multi-scale thermal analysis of GaAs RF device," in *Semiconductor Thermal Measurement and Management Symposium, 2005 IEEE Twenty First Annual IEEE*, 2005, pp. 259-263.

[3] R. S. Pengelly, S. M. Wood, J. W. Milligan, S. T. Sheppard, and W. L. Pribble, "A review of GaN on SiC high electron-mobility power transistors and MMICs," *IEEE Transactions on Microwave Theory and Techniques,* vol. 60, pp. 1764-1783, 2012.

[4] M. Kuball and J. W. Pomeroy, "A Review of Raman Thermography for Electronic and Opto-Electronic Device Measurement With Submicron Spatial and Nanosecond Temporal Resolution," *IEEE Transactions on Device and Materials Reliability,* vol. 16, pp. 667-684, 2016.

[5] A. Sarua, H. Ji, M. Kuball, M. J. Uren, T. Martin, K. P. Hilton, *et al.*, "Integrated micro-Raman/infrared thermography probe for monitoring of self-heating in AlGaN/GaN transistor structures," *IEEE Transactions on Electron Devices,* vol. 53, pp. 2438-2447, 2006.

[6] G. Pavlidis, D. Mele, T. Cheng, F. Medjdoub, and S. Graham, "The thermal effects of substrate removal on GaN HEMTs using Raman Thermometry," in *Thermal and Thermomechanical Phenomena in Electronic Systems (ITherm), 2016 15th IEEE Intersociety Conference on*, 2016, pp. 1255-1260.

[7] S. Martin-Horcajo, J. W. Pomeroy, B. Lambert, H. Jung, H. Blanck, and M. Kuball, "Transient Thermoreflectance for Gate Temperature Assessment in Pulse Operated GaN-Based HEMTs," *IEEE Electron Device Letters,* vol. 37, pp. 1197-1200, 2016.

[8] O. Lancry, E. Pichonat, J. Réhault, M. Moreau, R. Aubry, and C. Gaquière, "Development of time-resolved UV micro-Raman

spectroscopy to measure temperature in AlGaN/GaN HEMTs," *Solid-State Electronics,* vol. 54, pp. 1434-1437, 2010.

[9] R. B. Simon, J. W. Pomeroy, and M. Kuball, "Diamond micro-Raman thermometers for accurate gate temperature measurements," *Applied Physics Letters,* vol. 104, p. 213503, 2014.

[10] A. Shakouri, A. Ziabari, D. Kendig, J.-H. Bahk, Y. Xuan, D. Y. Peide, *et al.*, "Stable thermoreflectance thermal imaging microscopy with piezoelectric position control," in *Thermal Measurement, Modeling & Management Symposium (SEMI-THERM), 2016 32nd*, 2016, pp. 128-132.

[11] M. Farzaneh, K. Maize, D. Lüerßen, J. Summers, P. Mayer, P. Raad, *et al.*, "CCD-based thermoreflectance microscopy: principles and applications," *Journal of Physics D: Applied Physics,* vol. 42, p. 143001, 2009.

[12] A. Ziabari, J.-H. Bahk, Y. Xuan, D. Y. Peide, D. Kendig, K. Yazawa, *et al.*, "Sub-diffraction limit thermal imaging for HEMT devices," in *Thermal Measurement, Modeling & Management Symposium (SEMI-THERM), 2015 31st*, 2015, pp. 82-87.

[13] D. Pierścińska, "Thermoreflectance spectroscopy–Analysis of thermal processes in semiconductor lasers," *Journal of Physics D: Applied Physics,* 2017.

[14] Cree Inc. Appl. Note, "Thermal Performance Guide for High Power SiC MESFET and GaN HEMT Transistors ", 2013